70th International Astronautical Congress (IAC), Washington D.C., United States, 21-25 October 2019.

IAC-19-C1.6.2

Analytic Spacecraft Attitude and Rate Estimation Performance During Attitude Sensor Outages

Joseph M Galante[a]

[a] Attitude Control Systems Engineering Branch, NASA Goddard Space Flight Center, Greenbelt, MD, joseph.m.galante@nasa.gov

Abstract

Analytic expressions for spacecraft attitude and rate estimation performance of an attitude estimation filter in terms of sensor specifications are useful tools for spacecraft design. Farrenkopf (1978) famously found analytic expressions for steady-state pre-update and post-update attitude and gyro bias estimate error variances for an attitude estimation filter for a single-axis spacecraft with a Rate Output Gyro (ROG). Markley and Reynolds (2000) extended the analysis for a Rate-Integrating Gyro (RIG) with angle white noise. These expressions allow for the rapid evaluation of system performance during preliminary mission design phases. One contribution of this paper is the analytic calculation of the steady-state pre-update and post-update angular rate estimate uncertainty for both the ROG and RIG cases. The primary contribution of this paper is the extension of the results for both the ROG and the RIG cases to the situation of an attitude sensor outage. This situation arises frequently in practice; for example when a star sensor's field of view is occluded, when a star sensor's readings are unreliable during a thruster burn that vibrates the spacecraft, or during star sensor outages due to radiation upsets. Analytic expressions for the attitude estimate uncertainty, gyro bias estimate uncertainty, and angular rate estimate uncertainty are given in terms of the attitude sensor outage interval, the star tracker measurement noise, and gyro noise parameters. Validity of the analytic results is demonstrated via Monte Carlo simulation.

Keywords: filter, gyro, spacecraft, performance, estimate

Acronyms

MEKF Multiplicative Extended Kalman Filter

RIG Rate-Integrating Gyro

ROG Rate Output Gyro

1 Introduction

Kalman filter techniques [1, 2, 3] have been widely utilized for spacecraft attitude estimation algorithms by fusing star tracker and gyro measurements [4, 5, 6]. When the spacecraft gyro is a Rate Output Gyro (ROG), Farrenkopf [7, 8] famously found analytic expressions for steady-state pre-update and post-update attitude and gyro bias estimate error variances for an attitude estimation filter for a single-axis spacecraft. Farrenkopf's analysis modeled a single-axis ROG as having an unstable bias and angle random walk noise. Farrenkopf's result is useful for preliminary analysis of spacecraft attitude estimation systems in terms of simple sensor noise specifications. Markley and Reynolds extended this analysis for the case of a Rate-Integrating Gyro (RIG) [9] which is modeled as having the additional noise source of angle white noise; the work lead to a derivation of a full three-axis attitude estimation filter for RIGs [10]. Farrenkopf's analysis was recently extended to consider various types of rate estimation in addition to attitude and gyro bias [11], but analytic expressions have yet to be developed and will not be considered in this paper.

In all of the above mentioned cases, analytical filter performance results were obtained for steady-state conditions where both the star tracker and gyro measurements are available. One contribution of this paper is the analytic calculation of the steady-state pre-update and post-update angular rate estimate uncertainty for both the ROG and RIG cases. However, it is also desirable to understand filter estimate performance during an attitude sensor outage. During an attitude sensor outage, the estimation algorithm's estimates must be propagated by the gyro alone. This situation arises frequently in practice; for example, when a star sensor's field of view is occluded, when a star sensor's readings are unreliable during a thruster burn the vibrates the spacecraft, or when a star sensor resets due to a radiation event. The primary contributions of this paper are the formulation of analytic expressions for the attitude estimate uncertainty, gyro bias estimate uncertainty, and angular rate estimate uncertainty in terms of the attitude sensor outage interval, the attitude sensor measurement noise, and gyro noise parameters.

This paper consists of two main parts. Section 2 presents the standard ROG model frequently used in the literature, reviews Farrenkopf's [7, 8] classic analysis, develops an expression for a rate estimate and its associated uncertainty, and finally extends the analysis to obtain algebraic expressions for the attitude, gyro bias, and rate estimate uncertainty as a function of attitude sensor outage time. The following Section 3 presents a RIG model, reviews Markley's and Reynolds' [9] analysis, develops an expression for a rate estimate and its associated uncertainty, and finally extends the analysis to obtain algebraic expressions for the attitude, gyro bias, and rate estimate uncertainty as a function of attitude sensor outage time.

2 Rate Output Gyro (ROG)

This section focuses on the case of a single-axis Rate Output Gyro (ROG). A ROG model is presented in Section 2.1. The ROG is then used in a single-axis attitude estimation filter 2.2 that estimates spacecraft attitude and gyro bias. Farrenkopf's famous analysis is reviewed in Section 2.3; additionally, a simple rate estimate is presented and an analytic expression for its uncertainty is developed. Section 2.4 formulates expressions for attitude, rate, and gyro bias estimates during an attitude sensor outage following steady-state operation. Finally, the analytic results are compared with numerical simulation in Section 2.5.

This system is of frequent interest as it is a single-axis analog to the full three-axis Multiplicative Extended Kalman Filter (MEKF) of [5, 6] commonly used on spacecraft. The analytic results from a single-axis analog allow for rapid evaluation of estimation performance for given hardware specifications and to provide data for validation of MEKF implementations in flight software.

2.1 Rate Output Gyro (ROG) Model

Farrenkopf [7, 8] considered the Rate Output Gyro (ROG) model

$$\omega_g(t) = \omega(t) + b(t) + \sigma_v n_v(t) \tag{1}$$

where $\omega_g(t)$ is the gyro measurement at time t, $\omega(t)$ is the true angular rate, and the angle random walk noise $\sigma_v n_v(\cdot)$ is a zero mean Gaussian white noise process with variance σ_v^2 such that

$$E\left[\sigma_v n_v(t)\sigma_v n_v(\tau)\right] = \sigma_v^2 \delta(t-\tau)$$

where $E[\cdot]$ is the expectation operator and $\delta(\cdot)$ is the Dirac delta function. The gyro measurement is further corrupted by a bias $b(t)$ which drifts according to the model

$$\dot{b}(t) = \sigma_u n_u(t) \tag{2}$$

where the bias drift noise $\sigma_u n_u(\cdot)$ is a zero mean Gaussian white noise process with variance σ_u^2 such that

$$E\left[\sigma_u n_u(t)\sigma_u n_u(\tau)\right] = \sigma_u^2 \delta(t-\tau)$$

The angle random walk noise is assumed to be independent of the bias drift noise, implying

$$E\left[\sigma_v n_v(t)\sigma_u n_u(\tau)\right] = 0$$

2.2 Single-Axis Attitude Filter for ROG

The rotational motion of a single-axis spacecraft is given by the trivial kinematic model

$$\dot{\theta}(t) = \omega(t) \tag{3}$$

which relates the spacecraft attitude $\theta(t)$ to its angular rate $\omega(t)$. The dynamics of spacecraft motion, namely the differential equation for $\dot{\omega}(t)$, may be difficult to characterize as they may depend on fuel slosh, structural flex, air drag, solar radiation pressure, gravity gradients, electrical dipole torques, and other sources. It is common to algebraically substitute the true angular rate in Equation 3 with the content of Equation 1, a modeling technique known as "dynamic model replacement" [4, 5, 6, 7, 8, 11]. Performing this substitution leads to the satellite kinematic model

$$\dot{\theta}(t) = \omega_g(t) - b(t) - \sigma_v n_v(t)$$

Combining the satellite kinematic model with the gyro bias drift relation of Equation 2 one can model the system with the state

$$\boldsymbol{x}(t) = \begin{bmatrix}\theta(t)\\ b(t)\end{bmatrix} \tag{4}$$

Assuming the gyro measurement ω_g is available with period Δt the system dynamics have the discrete time model [12, 13]

$$\boldsymbol{x}(t_{k+1}) = \Phi(\Delta t)\boldsymbol{x}(t_k) + \Gamma(\Delta t)\omega_g(t_k) + \boldsymbol{n}(t_k) \tag{5}$$

where for time step $\Delta t = t_{k+1} - t_k$ the state transition matrix is

$$\Phi(\Delta t) = \begin{bmatrix}1 & -\Delta t\\ 0 & 1\end{bmatrix}$$

the gyro input matrix is

$$\Gamma(\Delta t) = \begin{bmatrix}\Delta t\\ 0\end{bmatrix}$$

and

$$\boldsymbol{n}(t_k) = \begin{bmatrix}\int_{t_k-\Delta t}^{t_k}\left[-\sigma_v n_v(\tau) - (t_k-\tau)\,\sigma_u n_u(\tau)\right]d\tau\\ \int_{t_k-\Delta t}^{t_k}\sigma_v n_v(\tau)d\tau\end{bmatrix}$$

Taking the expectation of the process noise term $\boldsymbol{n}(t_k)$ with itself yields the process noise covariance

$$\begin{aligned}Q(\Delta t) &= E\left[\boldsymbol{n}(t_k)\boldsymbol{n}^T(t_k)\right]\\ &= \begin{bmatrix}\sigma_v^2\Delta t + \frac{1}{3}\sigma_u^2\Delta t^3 & -\frac{1}{2}\sigma_u^2\Delta t^2\\ -\frac{1}{2}\sigma_u^2\Delta t^2 & \sigma_u^2\Delta t\end{bmatrix}\end{aligned} \tag{6}$$

A single-axis attitude estimation filter for a ROG with a state given by Equation 4 will have a state covariance matrix of

$$P(t_k) = E[(\boldsymbol{x}(t_k) - \hat{\boldsymbol{x}}(t_k))\left(\boldsymbol{x}(t_k) - \hat{\boldsymbol{x}}(t_k)\right)^T]$$

where $\hat{\boldsymbol{x}}(t_k)$ is the filter's estimate of the true state $\boldsymbol{x}(t_k)$ at time t_k. The state estimate may be propagated from its value $\hat{\boldsymbol{x}}(t_k^+)$ just after the most recent attitude measurement update to its value $\hat{\boldsymbol{x}}(t_{k+1}^-)$ just before the next attitude measurement update by using the expectation of Equation 5:

$$\hat{\boldsymbol{x}}(t_{k+1}^-) = \Phi(\Delta t)\hat{\boldsymbol{x}}(t_k^+) + \Gamma(\Delta t)\omega_g(t_k)$$

where the gyro measurement $\omega_g(t_k)$ is used to propagate the system state estimate between attitude measurements. The state covariance matrix is propagated from its value of $P(t_k^+)$ just after the most recent attitude measurement update to its value $P(t_{k+1}^-)$ just before the next attitude measurement update using

$$P(t_{k+1}^-) = \Phi(\Delta t)P(t_k^+)\Phi^T(\Delta t) + Q(\Delta t) \tag{7}$$

Attitude measurements, from a star tracker or some other sensor, are modeled as

$$\begin{aligned} y(t_k) &= H\boldsymbol{x}(t_k) + \sigma_n n_n(t_k) \\ &= \theta(t_k) + \sigma_n n_n(t_k) \end{aligned} \tag{8}$$

where $y(t_k)$ is the attitude measurement at time t_k, the measurement matrix $H = [1\ 0]$, and the attitude measurement noise $\sigma_n n_n(\cdot)$ is a zero mean Gaussian white noise process with variance σ_n^2. The attitude measurement noise is assumed independent of all gyro measurement noise. The attitude measurement noise covariance matrix is simply

$$R = E[\sigma_n^2 n_n^2(t)] = \sigma_n^2$$

Given an attitude measurement $y(t_k)$ at time t_k, the state covariance is updated from $P(t_k^-)$ to $P(t_k^+)$ by applying the measurement information using the Kalman gain:

$$K(t_k) = P(t_k^-)H^T\left(HP(t_k^-)H^T + R\right)^{-1} \tag{9}$$

$$P(t_k^+) = P(t_k^-) - K(t_k)HP(t_k^-) \tag{10}$$

The system state estimate is also updated by the measurement information using the Kalman gain:

$$\hat{\boldsymbol{x}}(t_k^+) = \hat{\boldsymbol{x}}(t_k^-) + K(t_k)\left(y(t_k) - H\hat{\boldsymbol{x}}(t_k^-)\right)$$

2.3 Analytic Steady State Filter Uncertainty

Given that the process noise covariance matrix Q, the measurement noise covariance matrix R, and the state transition matrix Φ are all independent of the state, the dynamics of the filter's state covariance matrix $P(\cdot)$ may be studied exclusively via Equations 7, 9, and 10. As the system is observable, the state covariance matrix will converge asymptotically to a steady state limit. In other words, there is a time index j such that

$$P(t_{k+1}^-) \approx P(t_k^-) \tag{11}$$

$$P(t_{k+1}^+) \approx P(t_k^+) \tag{12}$$

for all $k > j$. Denote the limiting covariance matrices as

$$\begin{aligned} P(t_k^-) = P(-) &= \begin{bmatrix} \sigma_{\theta\theta}^2(-) & \sigma_{\theta b}^2(-) \\ \sigma_{\theta b}^2(-) & \sigma_{bb}^2(-) \end{bmatrix} \\ P(t_k^+) = P(+) &= \begin{bmatrix} \sigma_{\theta\theta}^2(+) & \sigma_{\theta b}^2(+) \\ \sigma_{\theta b}^2(+) & \sigma_{bb}^2(+) \end{bmatrix} \end{aligned} \tag{13}$$

Farrenkopf showed [7] that Equations 7, 9, 10, 11, and 12 reduce to the single quartic equation

$$x^4 + S_u^2 x^3 + S_u^2\left(\frac{1}{6}S_u^2 - S_v^2 - 2\right)x^2 + S_u^4 x + S_u^4 = 0$$

where

$$\begin{aligned} S_u &= \frac{\sigma_u \Delta t^{3/2}}{\sigma_n} \\ S_v &= \frac{\sigma_v\sqrt{\Delta t}}{\sigma_n} \\ x &= \frac{\sigma_{\theta b}^2(-)\Delta t}{\sigma_n^2} \end{aligned} \tag{14}$$

and Δt is the time between attitude measurements.

Farrenkopf later [8] found a unique analytic solution to the quartic equation by discarding non-physical solutions. Farrenkopf found

$$\sigma_{\theta\theta}(-) = \sigma_n\sqrt{\left(\frac{x}{S_u}\right)^2 - 1} \tag{15}$$

$$\sigma_{\theta\theta}(+) = \sigma_n\sqrt{1 - \left(\frac{S_u}{x}\right)^2} \tag{16}$$

$$\sigma_{bb}(-) = \frac{\sigma_n}{\Delta t}\sqrt{S_u^2\left(\frac{1}{x} + \frac{1}{2}\right) - x} \tag{17}$$

$$\sigma_{bb}(+) = \frac{\sigma_n}{\Delta t}\sqrt{S_u^2\left(\frac{1}{x} - \frac{1}{2}\right) - x} \tag{18}$$

where

$$\begin{aligned} \beta &= \sqrt{S_u^2\left(4 + S_v^2\right) + \frac{S_u^4}{12}} \\ x &= -\frac{1}{2}\left[\left(\frac{S_u^2}{2} + \beta\right) + \sqrt{\left(\frac{S_u^2}{2} + \beta\right)^2 - 4S_u^2}\right] \end{aligned}$$

Trivial algebraic manipulation of Equation 14 yields the solution for $\sigma_{\theta b}^2(-)$

$$\sigma_{\theta b}^2(-) = \frac{\sigma_n^2}{\Delta t}x$$

Using the solution for all elements of $P(-)$ and algebraic substitution into Equations 9 and 10 further yield

$$\sigma^2_{\theta b}(+) = -\frac{S_u^2 \sigma_n^2}{\Delta tx} \quad (19)$$

An estimate of the angular rate at time t_k^- can be computed by subtracting the filter's bias estimate from the gyro measurement

$$\hat{\omega}(t_k^-) = \omega_g(t) - \hat{b}(t_k^-) \quad (20)$$

The rate estimate uncertainty at time t_k^- is then

$$\begin{aligned}
\sigma^2_{\omega\omega}(-) &= E\left[\left(\omega(t_k) - \hat{\omega}(t_k^-)\right)^2\right] \\
&= E\left[\left(-\left(b(t_k) - \hat{b}(t_k^-)\right) - \sigma_v n_v(t_k)\right)^2\right] \\
&= E\left[\left(b(t_k) - \hat{b}(t_k^-)\right)^2\right] + E\left[\sigma_v^2 n_v^2(t_k)\right] \\
&\quad + 2E\left[\left(b(t_k) - \hat{b}(t_k^-)\right)\sigma_v n_v(t_k)\right] \\
&= \sigma^2_{bb}(-) + \sigma_v^2 \quad (21)
\end{aligned}$$

where the fact that $\left(b(t_k) - \hat{b}(t_k^-)\right)$ is independent of $n_v(t_k)$ was used. Similarly, the uncertainty in this rate estimate just after a bias estimate update (at time t_k^+) is

$$\sigma^2_{\omega\omega}(+) = E\left[\left(\omega(t_k) - \hat{\omega}(t_k^+)\right)^2\right] = \sigma^2_{bb}(+) + \sigma_v^2$$

2.4 Analytic Estimate Uncertainty after Propagation

Now consider the case when the filter has reached steady state and then the attitude measurements suddendly become unavailable. Denote the time of the most recent attitude measurement as t_{ss}. After processing this attitude measurement, the state covariance matrix has value

$$P(t_{ss}^+) = P(+) = \begin{bmatrix} \sigma^2_{\theta\theta}(+) & \sigma^2_{\theta b}(+) \\ \sigma^2_{\theta b}(+) & \sigma^2_{bb}(+) \end{bmatrix}$$

where $\sigma^2_{\theta\theta}(+)$, $\sigma^2_{\theta b}(+)$, and $\sigma^2_{bb}(+)$ are given by Equations 16, 19, and 18 of the previous section.

After the attitude measurements become unavailable, the only thing the filter can do is to propagate its solution using gyro measurements. The remainder of this section will develop analytic expressions for the attitude estimate uncertainty, gyro bias estimate uncertainty, and angular rate estimate uncertainty as a function of the time elapsed since the filter was at steady state.

Consider the time $t_p > t_{ss}$. At this time the filter has propagated its state estimates $\Delta t_p = t_p - t_{ss}$ seconds since the most recent attitude update at t_{ss}. The state covariance matrix $P(t_p^-)$ at propagation time t_p^- is found by propagating $P(t_{ss}^+)$ according to the usual equation

$$\begin{aligned}
P(t_p^-) &= \begin{bmatrix} \sigma^2_{\theta\theta}(t_p^-) & \sigma^2_{\theta b}(t_p^-) \\ \sigma^2_{\theta b}(t_p^-) & \sigma^2_{bb}(t_p^-) \end{bmatrix} \\
&= \Phi(\Delta t_p) P(t_{ss}^+) \Phi^T(\Delta t_p) + Q(\Delta t_p) \quad (22)
\end{aligned}$$

where

$$\Phi(\Delta t_p) = \begin{bmatrix} 1 & -\Delta t_p \\ 0 & 1 \end{bmatrix}$$

and

$$Q(\Delta t_p) = \begin{bmatrix} \sigma_v^2 \Delta t_p + \frac{1}{3}\sigma_u^2 \Delta t_p^3 & -\frac{1}{2}\sigma_u^2 \Delta t_p^2 \\ -\frac{1}{2}\sigma_u^2 \Delta t_p^2 & \sigma_u^2 \Delta t_p \end{bmatrix}$$

Evaluating the covariance propagation of Equation 22 yields

$$\begin{aligned}
\sigma^2_{\theta\theta}(t_p^-) &= \sigma^2_{\theta\theta}(+) - 2\Delta t_p \sigma^2_{\theta b}(+) + \Delta t_p^2 \sigma^2_{bb}(+) \\
&\quad + \sigma_v^2 \Delta t_p + \frac{1}{3}\sigma_u^2 \Delta t_p^3 \quad (23) \\
\sigma^2_{\theta b}(t_p^-) &= \sigma^2_{\theta b}(+) - \Delta t_p \sigma^2_{bb}(+) - \frac{1}{2}\sigma_u^2 \Delta t_p^2 \\
\sigma^2_{bb}(t_p^-) &= \sigma^2_{bb}(+) + \sigma_u^2 \Delta t_p \quad (24)
\end{aligned}$$

The rate estimate uncertainty at time t_p^- is

$$\sigma^2_{\omega\omega}(t_p^-) = E\left[\left(\omega(t_p) - \hat{\omega}(t_p^-)\right)^2\right] = \sigma^2_{bb}(t_p^-) + \sigma_v^2 \quad (25)$$

2.5 Numerical Simulation of ROG Single-Axis Filter

Consider a ROG with

$$\begin{aligned}
\sigma_v &= 43.6 \frac{\mu rad}{\sqrt{s}} = 9.00 \frac{arcsec}{\sqrt{s}} = 0.150 \frac{deg}{\sqrt{hr}} \\
\sigma_u &= 0.0404 \frac{\mu rad}{\sqrt{s^3}} = 0.00833 \frac{arcsec}{\sqrt{s^3}} = 0.500 \frac{deg}{\sqrt{hr^3}}
\end{aligned}$$

which is characteristic of a high-end MEMS gyro popular in CubeSats and SmallSats. Suppose star tracker measurements are available every 0.5 *sec* and have measurement noise

$$\sigma_n = 24.2\ \mu rad = 5.00\ arcsec = 0.00139\ deg$$

which is characteristic of high-end star trackers for CubeSats and SmallSats.

Assume a single axis spacecraft uses an attitude filter as described in Section 2.2 and has reached steady state operation. The filter's estimate uncertainty has been assessed in Section 2.3. Then assume the attitude measurements from the star tracker are suddenly unavailable, but the ROG is still used to propagate the filter's state estimates. The analysis of Section 2.4 provides analytic expressions for the filter uncertainty as a function of propagation time.

A Monte-Carlo simulation analysis was performed to demonstrate the predictive accuracy of the analytic results. The simulation analysis consists of 100 disctinct simulation realizations of the system with initial condition specified by the steady-state filter covariance matrix of Equation 13. In each realization the filter then uses a gyro only to propagate its estimates as star tracker measurements are assumed to be unavailable. The attitude estimate uncertainty growth is shown in Figure 1 where the grey trajectories are filter attitude estimate error realizations and the blue curves are $\pm 3\sigma_{\theta\theta}(t_p^-)$ from Equation 23. Gyro bias estimate errors are shown in Figure 2. Rate estimates from Equation 20 have errors shown in Figure 3.

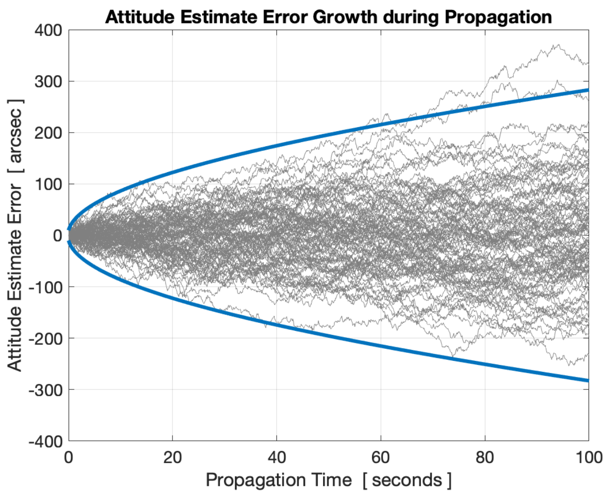

Figure 1: ROG filter attitude estimate error; grey trajectories are from 100 distinct simulation realizations, blue curves are $\pm 3\sigma_{\theta\theta}(t_p^-)$ analytic estimates from Equation 23.

3 Rate-Integrating Gyro (RIG)

This section focuses on the case of a single-axis Rate-Integrating Gyro (RIG). A RIG model is presented in Section 3.1. The RIG is then used in a single-axis attitude estimation filter 3.2 that estimates spacecraft attitude and gyro bias. Markley's and Reynolds' analysis is reviewed in Section 3.3; additionally, a simple rate estimate is presented and an analytic expression for its uncertainty is developed. Section 3.4 formulates expressions for attitude, rate, and gyro bias estimates during an attitude sensor outage following steady-state operation. Finally, the analytic results are compared with numerical simulation in Section 3.5.

This system is of frequent interest as it is a single-axis analog to the full three-axis Multiplicative Extended Kalman Filter (MEKF) extension for RIGs of [10]. As in the ROG case, the analytic results from a single-axis analog allow for rapid evaluation of estimation performance for given hardware specifications and to provide data for validation of MEKF implementations in flight software.

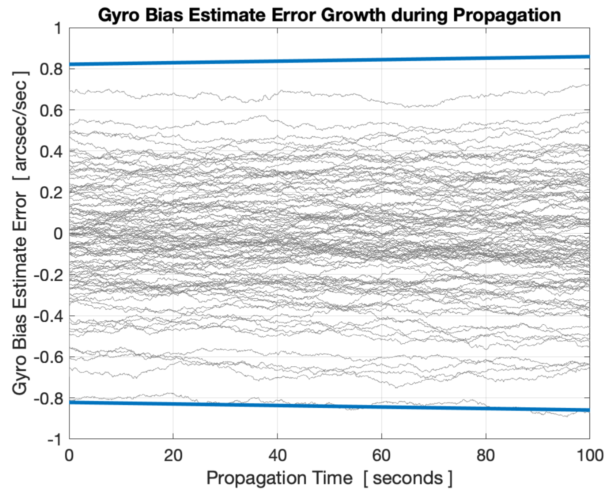

Figure 2: ROG filter gyro bias estimate error; grey trajectories are from 100 distinct simulation realizations, blue curves are $\pm 3\sigma_{bb}(t_p^-)$ analytic estimates from Equation 24.

3.1 Rate-Integrating Gyro (RIG) Model

Markley and Reynolds [9] considered the following model for a Rate-Integrating Gyro (RIG)

$$\dot{\phi}(t) = \omega(t) + b(t) + \sigma_v n_v(t) \quad (26)$$

where $\phi(t)$ is a dynamical state internal to the RIG. Assuming no bias $b(\cdot)$ and no angle random walk noise $\sigma_v n_v(\cdot)$, the RIG internal angle state $\phi(\cdot)$ would integrate the true spacecraft angular rate $\omega(t)$ to perfectly track change in the spacecraft attitude $\theta(t)$. RIGs typically do have angle random walk noise $\sigma_v n_v(\cdot)$, which is modeled as a zero mean Gaussian white noise process with variance σ_v^2 such that

$$E\left[\sigma_v n_v(t)\sigma_v n_v(\tau)\right] = \sigma_v^2 \delta(t-\tau)$$

just as in the ROG case. Similarly, the RIG is corrupted by a bias $b(t)$ which is assumed to drift according to the model

$$\dot{b}(t) = \sigma_u n_u(t) \quad (27)$$

where the bias drift noise $\sigma_u n_u(\cdot)$ is a zero mean Gaussian white noise process with variance σ_u^2 such that

$$E\left[\sigma_u n_u(t)\sigma_u n_u(\tau)\right] = \sigma_u^2 \delta(t-\tau)$$

The RIG output angle at time t_k is modeled as

$$\phi_g(t_k) = \phi(t_k) + \sigma_e n_e(t_k) \quad (28)$$

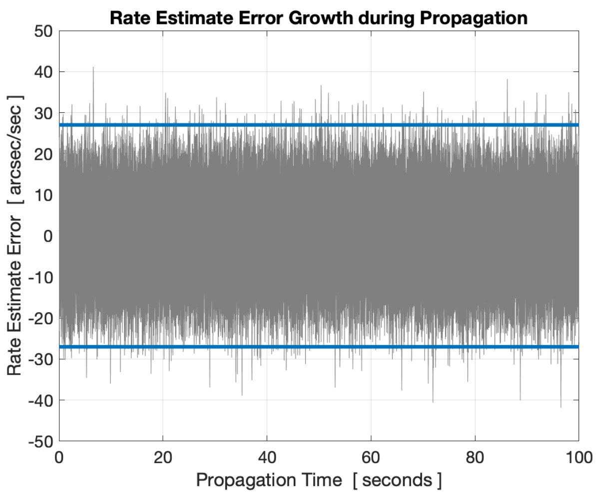

Figure 3: ROG filter rate estimate error; grey trajectories are from 100 distinct simulation realizations, blue curves are $\pm 3\sigma_{\omega\omega}(t_p^-)$ analytic estimates from Equation 25.

where the angle output noise $\sigma_e n_e(\cdot)$ is a zero mean Gaussian white noise process with variance σ_e^2 such that

$$E\left[\sigma_e n_e(t) \sigma_e n_e(\tau)\right] = \sigma_e^2 \delta(t-\tau)$$

Angle output noise is also known as readout noise and electronic noise.

The angle output noise, angle random walk noise, and bias drift noise are assumed to be independent of each other.

3.2 Single-Axis Attitude Filter for RIG

Combining the single-axis spacecraft kinematics model of Equation 3 with the RIG model of Equations 26 and 27 lead to the combined dynamics

$$\dot{\boldsymbol{x}}(t) = \begin{bmatrix} 0 & 0 & 0 \\ 0 & 0 & 0 \\ 0 & 1 & 0 \end{bmatrix} \boldsymbol{x}(t) + \begin{bmatrix} 1 \\ 0 \\ 1 \end{bmatrix} \omega(t) + \begin{bmatrix} 0 \\ \sigma_u n_u(t) \\ \sigma_v n_v(t) \end{bmatrix} \tag{29}$$

for the system state

$$\boldsymbol{x}(t) = \begin{bmatrix} \theta(t) \\ b(t) \\ \phi(t) \end{bmatrix} \tag{30}$$

The combined continuous time dynamics of Equation 29 can be discretized [9] allowing for the propagation of the state from time t_k to time $t_{k+1} = t_k + \Delta t$ via

$$\boldsymbol{x}(t_{k+1}) = \begin{bmatrix} 1 & 0 & 0 \\ 0 & 1 & 0 \\ 0 & \Delta t & 1 \end{bmatrix} \boldsymbol{x}(t_k) + \begin{bmatrix} 1 \\ 0 \\ 1 \end{bmatrix} u_{k+1} + \begin{bmatrix} 0 \\ \alpha_{k+1} \\ \beta_{k+1} \end{bmatrix} \tag{31}$$

where

$$u_{k+1} = \int_{t_k}^{t_{k+1}} \omega(\tau) d\tau$$

$$\alpha_{k+1} = \int_{t_k}^{t_{k+1}} \sigma_u n_u(\tau) d\tau$$

$$\beta_{k+1} = \int_{t_k}^{t_{k+1}} \sigma_v n_v(\tau) d\tau + \int_{t_k}^{t_{k+1}} (t_{k+1} - \tau)\, \sigma_u n_u(\tau) d\tau$$

Just as in Section 2.2, the "dynamic model replacement" technique is used to algebraically substitute the integral of the true angular rate in Equation 31 with the RIG measurement model of Equation 28. This substitution leads to the system dynamics model

$$\boldsymbol{x}(t_{k+1}) = \Phi(\Delta t) \boldsymbol{x}(t_k) + \begin{bmatrix} 1 \\ 0 \\ 1 \end{bmatrix} \phi_g(t_{k+1}) + \boldsymbol{n}(t_{k+1}) \tag{32}$$

where for $\Delta t = t_{k+1} - t_k$

$$\Phi(\Delta t) = \begin{bmatrix} 1 & -\Delta t & -1 \\ 0 & 1 & 0 \\ 0 & 0 & 0 \end{bmatrix} \tag{33}$$

$$\boldsymbol{n}(t_{k+1}) = \begin{bmatrix} -\beta_{k+1} - \sigma_e n_e(t_{k+1}) \\ \alpha_{k+1} \\ -\sigma_e n_e(t_{k+1}) \end{bmatrix}$$

Taking the expectation of the process noise term $\boldsymbol{n}(t_k)$ with itself yields the process noise covariance

$$\begin{aligned} Q(\Delta t) &= E\left[\boldsymbol{n}(t_k) \boldsymbol{n}^T(t_k)\right] \\ &= \begin{bmatrix} \sigma_v^2 \Delta t + \frac{1}{3}\sigma_u^2 \Delta t^3 + \sigma_e^2 & -\frac{1}{2}\sigma_u^2 \Delta t^2 & \sigma_e^2 \\ -\frac{1}{2}\sigma_u^2 \Delta t^2 & \sigma_u^2 \Delta t & 0 \\ \sigma_e^2 & 0 & \sigma_e^2 \end{bmatrix} \end{aligned} \tag{34}$$

whose upper left 2x2 block partition matches the ROG filter's process noise covariance matrix of Equation 6 when $\sigma_e = 0$.

A single-axis attitude estimation filter for a RIG with a state given by Equation 30 will have a state covariance matrix of

$$P(t_k) = E[(\boldsymbol{x}(t_k) - \hat{\boldsymbol{x}}(t_k))\,(\boldsymbol{x}(t_k) - \hat{\boldsymbol{x}}(t_k))^T]$$

where $\hat{\boldsymbol{x}}(t_k)$ is the filter's estimate of the true state $\boldsymbol{x}(t_k)$ at time t_k. The state estimate may be propagated from its value $\hat{\boldsymbol{x}}(t_k^+)$ just after the most recent attitude measurement update to its value $\hat{\boldsymbol{x}}(t_{k+1}^-)$ just before the next attitude measurement update by using the expectation of Equation 32:

$$\hat{\boldsymbol{x}}(t_{k+1}^-) = \Phi(\Delta t) \hat{\boldsymbol{x}}(t_k^+) + \begin{bmatrix} 1 \\ 0 \\ 1 \end{bmatrix} \phi_g(t_{k+1})$$

where the gyro measurement $\phi_g(t_{k+1})$ is used to propagate the system state estimate between attitude measurements. The state covariance matrix is propagated from its value of $P(t_k^+)$ just after the most recent attitude measurement update to its value $P(t_{k+1}^-)$ just before the next attitude measurement update using

$$P(t_{k+1}^-) = \Phi(\Delta t)P(t_k^+)\Phi^T(\Delta t) + Q(\Delta t) \tag{35}$$

which of course has exactly the same form as Equation 7; but note in the RIG case of Equation 35 the state covariance matrix $P(\cdot)$ has dimension 3x3, the 3x3 state transition matrix is given by Equation 33, and the 3x3 process noise covariance matrix is given by Equation 34.

Attitude measurements are modeled similarly to Equation 8 as

$$\begin{aligned} y(t_k) &= H\boldsymbol{x}(t_k) + \sigma_n n_n(t_k) \\ &= \theta(t_k) + \sigma_n n_n(t_k) \end{aligned} \tag{36}$$

where now in the RIG case $H = [1\ 0\ 0]$. As before, the attitude measurement noise covariance matrix is

$$R = E[\sigma_n^2 n_n^2(t)] = \sigma_n^2$$

Given an attitude measurement $y(t_k)$ at time t_k, the state covariance is updated from $P(t_k^-)$ to $P(t_k^+)$ by applying the measurement information using the Kalman gain:

$$K(t_k) = P(t_k^-)H^T\left(HP(t_k^-)H^T + R\right)^{-1} \tag{37}$$

$$P(t_k^+) = P(t_k^-) - K(t_k)HP(t_k^-) \tag{38}$$

The system state estimate is also updated by the measurement information using the Kalman gain:

$$\hat{\boldsymbol{x}}(t_k^+) = \hat{\boldsymbol{x}}(t_k^-) + K(t_k)\left(y(t_k) - H\hat{\boldsymbol{x}}(t_k^-)\right)$$

3.3 Analytic Steady State Filter Uncertainty

As in section 2.3, since the process noise covariance matrix Q, the measurement noise covariance matrix R, and the state transition matrix Φ are all independent of the state for the RIG case, the dynamics of the RIG filter's state covariance matrix $P(\cdot)$ may be studied exclusively via Equations 35, 37, and 38. The observable system dynamics again guarantee the state covariance matrix will converge asymptotically to a steady state limit; meaning there is a time index j such that

$$P(t_{k+1}^-) \approx P(t_k^-) \tag{39}$$

$$P(t_{k+1}^+) \approx P(t_k^+) \tag{40}$$

for all $k > j$. Denote the limiting covariance matrices as

$$P(t_k^-) = P(-) = \begin{bmatrix} \sigma_{\theta\theta}^2(-) & \sigma_{\theta b}^2(-) & \sigma_{\theta\phi}^2(-) \\ \sigma_{\theta b}^2(-) & \sigma_{bb}^2(-) & \sigma_{b\phi}^2(-) \\ \sigma_{\theta\phi}^2(-) & \sigma_{b\phi}^2(-) & \sigma_{\phi\phi}^2(-) \end{bmatrix} \tag{41}$$

$$P(t_k^+) = P(+) = \begin{bmatrix} \sigma_{\theta\theta}^2(+) & \sigma_{\theta b}^2(+) & \sigma_{\theta\phi}^2(+) \\ \sigma_{\theta b}^2(+) & \sigma_{bb}^2(+) & \sigma_{b\phi}^2(+) \\ \sigma_{\theta\phi}^2(+) & \sigma_{b\phi}^2(+) & \sigma_{\phi\phi}^2(+) \end{bmatrix} \tag{42}$$

Markley and Reynolds [9] showed that Equations 35, 37, 38, 39, and 40 reduce to the single quartic equation

$$\begin{aligned} &\left(\zeta^2 - 2\left(\gamma + \frac{1}{4}S_u\right)\zeta + 1 + S_e^2\right) \\ &\qquad \times \left(\zeta^2 + 2\left(\gamma - \frac{1}{4}S_u\right)\zeta + 1 + S_e^2\right) = 0 \end{aligned}$$

where

$$\begin{aligned} S_u &= \frac{\sigma_u \Delta t^{3/2}}{\sigma_n} \\ S_v &= \frac{\sigma_v \sqrt{\Delta t}}{\sigma_n} \\ S_e &= \frac{\sigma_e}{\sigma_n} \\ \sigma_{\theta b}^2(-) &= -\sigma_u\sigma_n\zeta\sqrt{\Delta t} \end{aligned}$$

and Δt is the time between attitude measurements.

Markley and Reynolds were able to analytically solve the quartic by discarding non-physical solutions. They found

$$\sigma_{\theta\theta}^2(-) = \left(\zeta^2 - 1\right)\sigma_n^2 \tag{43}$$

$$\sigma_{\theta\theta}^2(+) = \left(1 - \zeta^{-2}\right)\sigma_n^2 \tag{44}$$

$$\sigma_{bb}^2(-) = +\frac{1}{2}\Delta t\sigma_u^2 + \sigma_u\sqrt{2\gamma\sqrt{\Delta t}\sigma_u\sigma_n + \sigma_v^2 + \frac{1}{3}\Delta t^2\sigma_u^2} \tag{45}$$

$$\sigma_{bb}^2(+) = -\frac{1}{2}\Delta t\sigma_u^2 + \sigma_u\sqrt{2\gamma\sqrt{\Delta t}\sigma_u\sigma_n + \sigma_v^2 + \frac{1}{3}\Delta t^2\sigma_u^2} \tag{46}$$

$$\sigma_{\theta b}^2(-) = -\sigma_u\sigma_n\zeta\sqrt{\Delta t} \tag{47}$$

where

$$\begin{aligned} \gamma &= \sqrt{1 + S_e^2 + \frac{1}{4}S_v^2 + \frac{1}{48}S_u^2} \\ \zeta &= \gamma + \frac{1}{4}S_u + \frac{1}{2}\sqrt{2\gamma S_u + S_v^2 + \frac{1}{3}S_u^2} \end{aligned}$$

Note that Markley's and Reynolds' solution of Equations 43, 44, 45, and 46 for the RIG case only differ from Farrenkopf's solution of Equations 15, 16, 17, and 18 for the ROG case by the S_e term and notation. For $\sigma_e = 0$ the solutions are equivalent.

Solving for the remaining terms in the steady state covariance matrices, one can find

$$\begin{aligned}
\sigma^2_{\theta\phi}(-) &= \sigma_e^2 \\
\sigma^2_{b\phi}(-) &= 0 \\
\sigma^2_{\phi\phi}(-) &= \sigma_e^2 \\
\sigma^2_{\theta b}(+) &= -\frac{\sigma_u\sigma_n\sqrt{\Delta t}}{\zeta} \\
\sigma^2_{\theta\phi}(+) &= \frac{\sigma_e^2}{\zeta^2} \\
\sigma^2_{b\phi}(+) &= \frac{\sigma_u\sigma_e^2\sqrt{\Delta t}}{\sigma_n\zeta} \\
\sigma^2_{\phi\phi}(+) &= \sigma_e^2 - \frac{\sigma_e^4}{\sigma_n^2\zeta^2}
\end{aligned}$$

An estimate of the angular rate at time t_k^- can be formulated by back-differencing gyro measurement and subtracting the gyro bias estimate

$$\hat{\omega}(t_k^-) = \frac{\phi_g(t_k) - \phi_g(t_{k-1})}{\Delta t} - \hat{b}(t_{k-1}^-) \tag{48}$$

The error of this estimate is defined by $\tilde{\omega}(t_k^-) = \omega(t_k) - \hat{\omega}(t_k^-)$. To compute the error, first note that substitution of Equation 31 into 28 yields

$$\begin{aligned}
\phi_g(t_k) &= \Delta t b(t_{k-1}) + \phi(t_{k-1}) + \int_{t_{k-1}}^{t_k}\omega(\tau)d\tau + \sigma_e n_e(t_k) \\
&+ \int_{t_{k-1}}^{t_k}\sigma_v n_v(\tau)d\tau + \int_{t_{k-1}}^{t_k}(t_k-\tau)\sigma_u n_u(\tau)d\tau
\end{aligned}$$

Combining the above with Equation 28 again and writing the bias estimation error as $\tilde{b}(t_{k-1}^-) = b(t_{k-1}) - \hat{b}(t_{k-1}^-)$ results in the estimate error

$$\begin{aligned}
\tilde{\omega}(t_k^-) &= \left(\omega(t_k) - \frac{\int_{t_{k-1}}^{t_k}\omega(\tau)d\tau}{\Delta t}\right) - \tilde{b}(t_{k-1}^-) \\
&- \frac{1}{\Delta t}\int_{t_{k-1}}^{t_k}\sigma_v n_v(\tau)d\tau - \frac{1}{\Delta t}\int_{t_{k-1}}^{t_k}(t_k-\tau)\sigma_u n_u(\tau)d\tau \\
&- \frac{1}{\Delta t}\sigma_e n_e(t_k) + \frac{1}{\Delta t}\sigma_e n_e(t_{k-1})
\end{aligned}$$

where the first term vanishes for spacecraft angular rates that are constant over the differencing interval Δt. Assuming the spacecraft angular rate is constant over the differencing interval, the rate estimate uncertainty at time t_k^- is then

$$\begin{aligned}
\sigma^2_{\omega\omega}(-) &= E\left[\tilde{\omega}^2(t_k^-)\right] \\
&= \sigma^2_{bb}(-) + \frac{1}{\Delta t}\sigma_v^2 + \frac{\Delta t}{3}\sigma_u^2 + \frac{2}{\Delta t}\sigma_e^2
\end{aligned}$$

Similarly, the uncertainty in this rate estimate just after a bias estimate update (at time t_k^+) is

$$\begin{aligned}
\sigma^2_{\omega\omega}(+) &= E\left[\tilde{\omega}^2(t_k^+)\right] \\
&= \sigma^2_{bb}(+) + \frac{1}{\Delta t}\sigma_v^2 + \frac{\Delta t}{3}\sigma_u^2 + \frac{2}{\Delta t}\sigma_e^2
\end{aligned}$$

3.4 Analytic Estimate Uncertainty after Propagation

Now consider the case when the filter has reached steady state and then the attitude measurements suddendly become unavailable. Denote the time of the most recent attitude measurement as t_{ss}. After processing this attitude measurement, the state covariance matrix has value

$$P(t_{ss}^+) = P(+) = \begin{bmatrix} \sigma^2_{\theta\theta}(+) & \sigma^2_{\theta b}(+) & \sigma^2_{\theta\phi}(+) \\ \sigma^2_{\theta b}(+) & \sigma^2_{bb}(+) & \sigma^2_{b\phi}(+) \\ \sigma^2_{\theta\phi}(+) & \sigma^2_{b\phi}(+) & \sigma^2_{\phi\phi}(+) \end{bmatrix}$$

whose entries were given in Section 3.3.

As in Section 2.4 for the ROG case, this section will develop analytic expressions for the attitude estimate uncertainty, gyro bias estimate uncertainty, and angular rate estimate uncertainty as a function of the time elapsed since the filter was at steady state for a RIG.

Consider the time $t_p > t_{ss}$. At this time the filter has propagated its state estimates $\Delta t_p = t_p - t_{ss}$ seconds since the most recent attitude update at t_{ss}. The state covariance matrix $P(t_p^-)$ at propagation time t_p^- is found by propagating $P(t_{ss}^+)$ according to the usual equation

$$\begin{aligned}
P(t_p^-) &= \begin{bmatrix} \sigma^2_{\theta\theta}(t_p^-) & \sigma^2_{\theta b}(t_p^-) & \sigma^2_{\theta\phi}(t_p^-) \\ \sigma^2_{\theta b}(t_p^-) & \sigma^2_{bb}(t_p^-) & \sigma^2_{b\phi}(t_p^-) \\ \sigma^2_{\theta\phi}(t_p^-) & \sigma^2_{b\phi}(t_p^-) & \sigma^2_{\phi\phi}(t_p^-) \end{bmatrix} \\
&= \Phi(\Delta t_p)P(t_{ss}^+)\Phi^T(\Delta t_p) + Q(\Delta t_p)
\end{aligned} \tag{49}$$

where

$$\Phi(\Delta t_p) = \begin{bmatrix} 1 & -\Delta t_p & -1 \\ 0 & 1 & 0 \\ 0 & 0 & 0 \end{bmatrix}$$

and

$$Q(\Delta t_p) = \begin{bmatrix} \sigma_v^2\Delta t_p + \frac{1}{3}\sigma_u^2\Delta t_p^3 + \sigma_e^2 & -\frac{1}{2}\sigma_u^2\Delta t_p^2 & \sigma_e^2 \\ -\frac{1}{2}\sigma_u^2\Delta t_p^2 & \sigma_u^2\Delta t_p & 0 \\ \sigma_e^2 & 0 & \sigma_e^2 \end{bmatrix}$$

Evaluating the covariance propagation of Equation 49 yields

$$\begin{aligned}
\sigma^2_{\theta\theta}(t_p^-) &= \sigma^2_{\theta\theta}(+) + \Delta t_p^2\sigma^2_{bb}(+) + \sigma^2_{\phi\phi}(+) \\
&\quad - 2\Delta t_p\sigma^2_{\theta b}(+) - 2\sigma^2_{\theta\phi}(+) + 2\Delta t_p\sigma^2_{b\phi}(+) \\
&\quad + \Delta t_p\sigma_v^2 + \frac{1}{3}\Delta t_p^3\sigma_u^2 + \sigma_e^2
\end{aligned} \tag{50}$$

$$\begin{aligned}
\sigma^2_{\theta b}(t_p^-) &= \sigma^2_{\theta b}(+) - \Delta t_p\sigma^2_{bb}(+) - \sigma^2_{b\phi}(+) - \frac{1}{2}\Delta t_p^2\sigma_u^2 \\
\sigma^2_{\theta\phi}(t_p^-) &= \sigma_e^2 \\
\sigma^2_{bb}(t_p^-) &= \sigma^2_{bb}(+) + \Delta t_p\sigma_u^2 \\
\sigma^2_{b\phi}(t_p^-) &= 0 \\
\sigma^2_{\phi\phi}(t_p^-) &= \sigma_e^2
\end{aligned} \tag{51}$$

The spacecraft angular rate can be estimated similar to Equation 48, where the gyro bias estimate $\hat{b}(t_p^-)$ is used to correct successive gyro measurements in

$$\hat{\omega}(t_p^-) = \frac{\phi_g(t_j^-) - \phi_g(t_p^-)}{t_j - t_p} - \hat{b}(t_p^-) \quad (52)$$

where $t_j > t_p > t_{ss}$. Let $\Delta t_j = t_j - t_p$. The error in this estimate is then

$$\tilde{\omega}(t_j^-) = \left(\omega(t_j) - \frac{\int_{t_p}^{t_j} \omega(\tau) d\tau}{\Delta t}\right) - \tilde{b}(t_p^-) - \frac{1}{\Delta t_j}\int_{t_p}^{t_j} \sigma_v n_v(\tau) d\tau - \frac{1}{\Delta t_j}\int_{t_p}^{t_j} (t_j - \tau)\sigma_u n_u(\tau) d\tau - \frac{1}{\Delta t_j}\sigma_e n_e(t_k) + \frac{1}{\Delta t_j}\sigma_e n_e(t_{k-1})$$

where $\tilde{b}(t_p^-) = b(t_p) - \hat{b}(t_p^-)$. Assuming the spacecraft angular rate is constant over the differencing interval $t_p \leq t \leq t_j$, the rate estimate uncertainty at time t_j^- is

$$\sigma_{\omega\omega}^2(-) = E\left[\tilde{\omega}^2(t_j^-)\right] = \sigma_{bb}^2(t_p^-) + \frac{1}{\Delta t_j}\sigma_v^2 + \frac{\Delta t_j}{3}\sigma_u^2 + \frac{2}{\Delta t_j}\sigma_e^2 \quad (53)$$

3.5 Numerical Simulation of RIG Single-Axis Filter

Consider a RIG with

$$\sigma_v = 1.45\ \frac{\mu rad}{\sqrt{s}} = 0.300\ \frac{arcsec}{\sqrt{s}} = 0.00500\ \frac{deg}{\sqrt{hr}}$$

$$\sigma_u = 0.000404\ \frac{\mu rad}{\sqrt{s^3}} = 0.000083\ \frac{arcsec}{\sqrt{s^3}} = 0.00500\ \frac{deg}{\sqrt{hr^3}}$$

$$\sigma_e = 0.484814\ \mu rad = 0.100\ arcsec = 0.000028\ deg$$

which is characteristic of a Ring Laser Gyro common in large science satellites. Suppose star tracker measurements are available every 0.2 sec and have measurement noise

$$\sigma_n = 15.0\ \mu rad = 3.09\ arcsec = \ 0.000859 deg$$

which is characteristic of the navigation suite for these types of satellites.

As before, assume a single axis spacecraft uses an attitude filter as described in Section 3.2 and has reached steady state operation. The filter's estimate uncertainty has been assessed in Section 3.3. Then assume the attitude measurements from the star tracker are suddenly unavailable, but the RIG is still used to propagate the filter's state estimates. The analysis of Section 3.4 provides analytic expressions for the filter uncertainty as a function of propagation time.

A Monte-Carlo simulation analysis was performed to demonstrate the predictive accuracy of the analytic results. The simulation analysis consists of 100 disctinct simulation realizations of the system with initial condition specified by the steady-state filter covariance matrix of Equation 42. In each realization the filter then uses a gyro only to propagate its estimates as star tracker measurements are assumed to be unavailable. The attitude estimate uncertainty growth is shown in Figure 4 where the grey trajectories are filter attitude estimate error realizations and the blue curves are $\pm 3\sigma_{\theta\theta}(t_p^-)$ from Equation 50. Gyro bias estimate errors are shown in Figure 5. Rate estimates from Equation 52 have errors shown in Figure 6.

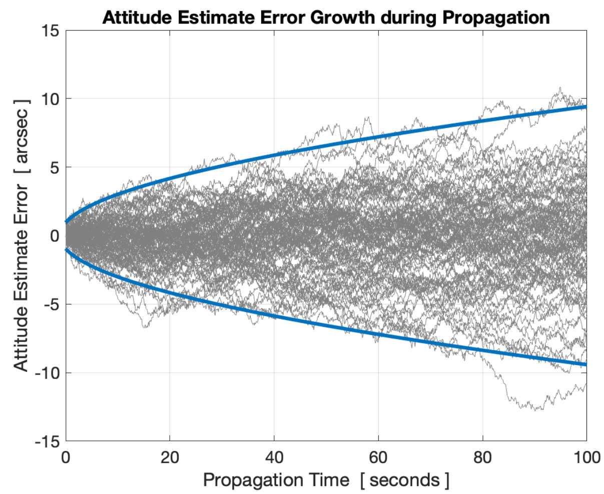

Figure 4: RIG filter attitude estimate error; grey trajectories are from 100 distinct simulation realizations, blue curves are $\pm 3\sigma_{\theta\theta}(t_p^-)$ analytic estimates from Equation 50.

4 Conclusion

Standard models for single-axis Rate Output Gyros (ROGs) and Rate-Integrating Gyros (RIGs) were presented. Single-axis attitue estimation filters were developed. The classic analysis of a single-axis spacecraft attitude estimator was presented; Farrenkopf's analysis [7, 8] for the ROG case and Markley's and Reynolds' [9] for the RIG case. This paper showed how these classic analyses may be used to find an analytic expression for uncertainty in a simple rate estimate. Finally, the analytic expressions for the uncertainty in attitude, gyro bias, and rate estimates as a function of propagation time were found for the situation when the spacecraft attitude estimator has reached steady-state operation and subsequently loses attitude measurements. Validity of the analytic results was demonstrated via Monte Carlo simulation.

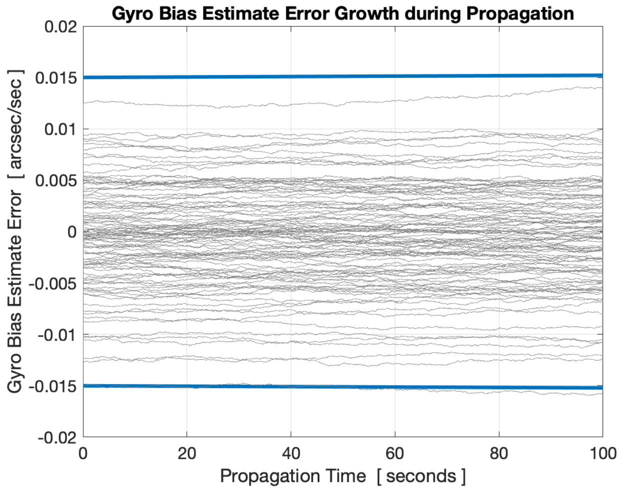

Figure 5: RIG filter gyro bias estimate error; grey trajectories are from 100 distinct simulation realizations, blue curves are $\pm 3\sigma_{bb}(t_p^-)$ analytic estimates from Equation 51.

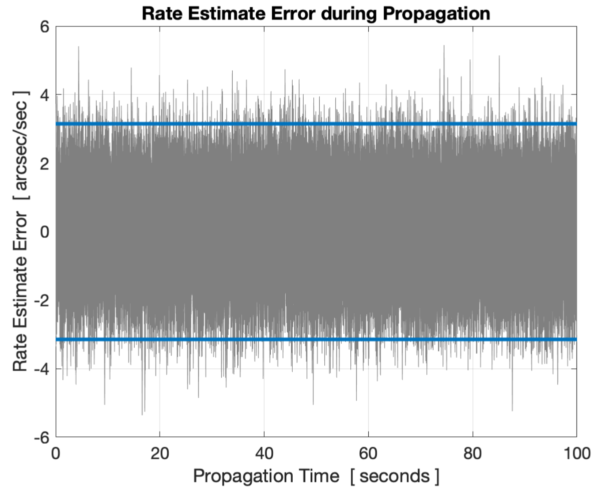

Figure 6: RIG filter rate estimate error; grey trajectories are from 100 distinct simulation realizations, blue curves are $\pm 3\sigma_{\omega\omega}(t_p^-)$ analytic estimates from Equation 53.

References

[1] R. E. Kalman, "A new approach to linear filtering and prediction problems," *Journal of basic Engineering*, vol. 82, no. 1, pp. 35–45, 1960.

[2] A. Gelb, *Applied Optimal Estimation.* MIT press, 1974.

[3] R. G. Brown and P. Y. Hwang, *Introduction to Random Signals and Applied Kalman Filtering.* New York, NY: John Wiley and Sons, 3rd ed., 1997.

[4] J. E. Potter and W. Vande, "Optimum mixing of gyroscope and star tracker data.," *Journal of Spacecraft and Rockets*, vol. 5, no. 5, pp. 536–540, 1968.

[5] E. J. Lefferts, F. L. Markley, and M. D. Shuster, "Kalman Filtering for Spacecraft Attitude Estimation," *Journal of Guidance, Control, and Dynamics*, vol. 5, no. 5, pp. 417–429, 1982.

[6] F. L. Markley, "Attitude Error Representations for Kalman Filtering," *Journal of Guidance, Control, and Dynamics*, vol. 26, no. 2, pp. 311–317, 2003.

[7] R. Farrenkopf, "Generalized results for precision attitude reference systems using gyros," in *Mechanics and Control of Flight Conference*, p. 903, 1974.

[8] R. Farrenkopf, "Analytic steady-state accuracy solutions for two common spacecraft attitude estimators," *Journal of Guidance and Control*, vol. 1, no. 4, pp. 282–284, 1978.

[9] F. L. Markley and R. Reynolds, "Analytic Steady-State Accuracy of a Spacecraft Attitude Estimator," *Journal of Guidance, Control, and Dynamics*, vol. 23, no. 6, pp. 1065–1067, 2000.

[10] J. L. Crassidis and F. L. Markley, "Three-axis attitude estimation using rate-integrating gyroscopes," *Journal of Guidance, Control, and Dynamics*, vol. 39, no. 7, pp. 1513–1526, 2016.

[11] A. D. Dianetti and J. L. Crassidis, "Extension of farrenkopf steady-state solutions with estimated angular rate," in *2018 AIAA Guidance, Navigation, and Control Conference*, p. 2095, 2018.

[12] J. L. Crassidis and J. L. Junkins, *Optimal Estimation of Dynamic Systems.* Chapman and Hall/CRC, 2011.

[13] F. L. Markley and J. L. Crassidis, *Fundamentals of Spacecraft Attitude Determination and Control.* Springer, 2014.